MÉTODOS NUMÉRICOS EN INGENIERÍA
R. Abascal, J. Domínguez y G. Bugeda (Eds.)

FINITE ELEMENT MODELLING OF THERMO-ELASTOPLASTIC BEHAVIOUR OF HOT-ROLLED STEEL PROFILES SUBMITTED TO FIRE

Fonseca, Elza M. M.*y Vila Real, Paulo M. M.†

* Departamento de Mecânica Aplicada
Instituto Politécnico de Bragança
Campus de Sta. Apolónia, apartado 134
5300 Bragança, Portugal
e-mail: efonseca@ipb.pt, Tel.: 351 73 3303094, Fax: 351 73 313051

† Departamento de Engenharia Civil
Universidade de Aveiro
Campus de Santiago
3810 Aveiro, Portugal
e-mail: pvreal@civil.ua.pt, Tel.: 351 34 370049, Fax: 351 34 370953

Key words: Fire, Thermo-elastoplasticity, Eurocodes, Heat Conduction, Non-Linearity, Standard temperature-time curve ISO 834, Finite Elements

Abstract. *This paper presents finite element algorithms developed to simulate the thermo-elastoplastic behaviour of steel profiles under high temperatures, in particular those arising from fire conditions. Transient analyses of the temperature field and the mechanical response at each instant have been done. The thermal response obtained with the finite element formulation and the results obtained using the simplified heat conduction equation according to the Eurocode 3 have been compared for several series of hot-rolled steel profiles. The non-linearity of the problem due to the thermal dependence of the material properties has been taken into account and an elastoplastic model has been used.*

1 INTRODUCTION

A finite element program FEMSEF98 – "Finite Element Modelling of Structures Exposed to Fire" has been developed to model the thermo-elastoplastic behaviour of hot-rolled steel profiles exposed to fire. Heat conduction is assumed for the heat transfer analysis and an elastoplastic model is employed to predict the development of thermal stresses and strains. In this paper the elastoplastic analysis is done using the Prandtl-Reuss's theory[1,8] for incremental plastic analysis.

A finite element formulation of the heat conduction in solids is presented, giving particular attention to the non-linearity of the problem. This non-linearity is treated by an iterative procedure based on the modified Newton-Raphson method, where in the original jacobian matrix the unysymmetric term is neglected[3].

The simplified heat conduction equation of the eurocode 3 is also non-linear wherefore an iterative procedure is also needed.

2 FORMULATION OF THERMO-ELASTOPLASTIC BEHAVIOUR

Neglecting the heat generated during the deformation, the thermal and the mechanical problems are uncoupled. So the technique involves concurrently solving an uncoupled set of equations, the transient heat conduction equation and the incremental equilibrium equation, within each time interval. The same finite element formulation (finite element mesh, shape function, etc.) and the same equation solution technique (frontal solution technique) are used in both the thermal and stress analysis.

2.1 Thermal analysis: the heat conduction equation and its boundary conditions

The governing equation for transient heat conduction in the domain Ω takes the form

$$\nabla(\lambda\nabla\theta) + \dot{Q} = \rho c_p \frac{\partial\theta}{\partial t} \tag{1}$$

where λ is the thermal conductivity, $\dot{Q}$ the heat generated/unit volume, ρ the density, c_p the specific heat, θ the temperature and t the time. The temperature field which satisfies eq. (1) in Ω, must satisfy the following boundary conditions: prescribed temperatures $\overline{\theta}$ on a part Γ_θ of the boundary; specified heat flux $\overline{q}$ on a part Γ_q of the boundary; heat flux by convection between a part Γ_c of the boundary at temperature θ, and the environment at the temperature θ_∞

$$q_c = h_c(\theta - \theta_\infty) \qquad \text{on } \Gamma_c \tag{2}$$

where h_c is the heat transfer coefficient by convection; heat flux by radiation between a part Γ_r of the boundary at the temperature θ and the environment at the absolute temperature θ_a

$$q_{\mathrm{r}} = \beta\varepsilon(\theta^4 - \theta_a^4) = \underbrace{\beta\varepsilon(\theta^2 + \theta_a^2)(\theta + \theta_a)}_{h_r}(\theta - \theta_a) = h_r(\theta - \theta_a) \qquad \text{on } \Gamma_r \tag{3}$$

where β is the Stefan-Boltzmann constant, ε is the emissivity and h_r is the heat transfer coefficient by radiation. If the heat flux is simultaneously by convection and radiation and if in particular $\theta_\infty = \theta_a$, we can write

$$q_{cr} = q_c + q_r = h_c(\theta - \theta_\infty) + h_r(\theta - \theta_a) = h_{cr}(\theta - \theta_\infty) \tag{4}$$

where $h_{cr} = h_c + h_r$ is the combined convection and radiation heat transfer coefficient.

2.1.1 Finite element discretization and time integration

Using finite elements Ω^e to discretize the domain Ω, a weak formulation and the Galerkin method for choosing the weighting functions, we obtain[2] the following system of differential equations

$$\mathbf{K}\boldsymbol{\theta} + \mathbf{C}\dot{\boldsymbol{\theta}} = \mathbf{F} \tag{5}$$

where

$$K_{lm} = \sum_{e=1}^{E} \int_{\Omega^e} \left(\nabla N_l \lambda \nabla N_m\right) d\Omega^e + \sum_{e=1}^{H} \int_{\Gamma_h^e} h_{cr} N_l N_m \, d\Gamma_h^e \tag{6}$$

$$C_{lm} = \sum_{e=1}^{E} \int_{\Omega^e} \rho c_p N_l N_m \, d\Omega^e \tag{7}$$

$$F_l = \sum_{e=1}^{E} \int_{\Omega^e} N_l \dot{Q} \, d\Omega^e - \sum_{e=1}^{Q} \int_{\Gamma_q^e} N_l \overline{q} \, d\Gamma_q^e + \sum_{e=1}^{H} \int_{\Gamma_h^e} N_l h_{cr} \theta_\infty \, d\Gamma_h^e \tag{8}$$

where E is the total number of elements, Q is the number of elements with boundary type Γ_q, H is the number of elements with boundary type Γ_c and/or Γ_r, N_l and N_m are shape functions.

Using a finite difference technique to discretize the time, the system of ordinary differential equations (5) results in the recurrence formula:

$$\hat{\mathbf{K}}_{n+\alpha} \boldsymbol{\theta}_{n+\alpha} = \hat{\mathbf{F}}_{n+\alpha} \qquad 0 < \alpha \le 1 \tag{9}$$

where

$$\hat{\mathbf{K}}_{n+\alpha} = \mathbf{K}_{n+\alpha} + \frac{1}{\alpha\,\Delta t} \mathbf{C}_{n+\alpha} \tag{10}$$

$$\hat{\mathbf{F}}_{n+\alpha} = \mathbf{F}_{n+\alpha} + \frac{1}{\alpha \Delta t} \mathbf{C}_{n+\alpha} \boldsymbol{\theta}_n \tag{11}$$

Having solved the system of equations (9) for $\boldsymbol{\theta}_{n+\alpha}$, at time $t_{n+\alpha}$, the value of $\boldsymbol{\theta}$ at the end of the time interval Δt, that is, at time t_{n+1} is given by

$$\boldsymbol{\theta}_{n+1} = \frac{1}{\alpha}\boldsymbol{\theta}_{n+\alpha} + \left(1 - \frac{1}{\alpha}\right)\boldsymbol{\theta}_n \tag{12}$$

Varying the value of the parameter α, we can obtain several time integration schemes[2], like the *Crank-Nicolson scheme* for $\alpha = 1/2$, the *Galerkin scheme* for $\alpha = 2/3$ and the *Euler Backward scheme* for $\alpha = 1$.

2.1.2 Iterative procedure for the solution of the non-linear thermal transient problem

In non-linear problems, where the thermal properties of the material are temperature dependent, the system of equations (5) can generally be written as

$$\mathbf{K}(\boldsymbol{\theta},t)\boldsymbol{\theta}(t) + \mathbf{C}(\boldsymbol{\theta},t)\dot{\boldsymbol{\theta}}(t) = \mathbf{F}(\boldsymbol{\theta},t) \tag{13}$$

There is not a general method to solve this system of non-linear differential equations. However, several numerical solution procedures, in essence, based on a linear time integration and an iterative process are available[2,3,4,5,6]. Here, an effective algorithm for the analysis of non-linear transient thermal problem is presented. The matrices **K** and **C** and the vector **F**, needed to construct $\hat{\mathbf{K}}_{n+\alpha}$ and $\hat{\mathbf{F}}_{n+\alpha}$, given by eq. (10) and (11), can vary throughout the time interval Δt as functions of the unknown vector temperature θ and time *t*. Therefore, these matrices must be evaluated at time $t_{n+\alpha}$ and the temperature $\theta_{n+\alpha}$, so that

$$\mathbf{K}_{n+\alpha} = \mathbf{K}(\boldsymbol{\theta}_{n+\alpha}, t_{n+\alpha}) \tag{14}$$

$$\mathbf{K}_{n+\alpha} = \mathbf{K}(\boldsymbol{\theta}_{n+\alpha}, t_{n+\alpha}) \tag{15}$$

$$\mathbf{K}_{n+\alpha} = \mathbf{K}(\boldsymbol{\theta}_{n+\alpha}, t_{n+\alpha}) \tag{16}$$

In order to fully satisfy these non-linear conditions of the problem, it is necessary to employ an iterative procedure in each time step. In this algorithm a modified Newton-Raphson method is adopted[3,4,5]. During any step, *i*, of the iterative process of solution, eq. (9) will not generally be satisfied unless convergence has occurred. Therefore a system of residual *forces* ψ will exist, so that

$$\boldsymbol{\psi}^i_{n+\alpha} = \hat{\mathbf{F}}^i_{n+\alpha} - \hat{\mathbf{K}}^i_{n+\alpha}\boldsymbol{\theta}^{i+1}_{n+\alpha} \neq 0 \tag{17}$$

The improved value of $\boldsymbol{\theta}^{i+1}_{n+\alpha}$ can be obtained by

$$\Delta\boldsymbol{\theta}^i_{n+\alpha} = \left[\hat{\mathbf{K}}^i_{n+\alpha}\right]^{-1}\boldsymbol{\psi}^i_{n+\alpha} \tag{18}$$

and

$$\boldsymbol{\theta}_{n+\alpha}^{i+1} = \boldsymbol{\theta}_{n+\alpha}^{i} + \Delta\boldsymbol{\theta}_{n+\alpha}^{i} \tag{19}$$

The iterative procedure is then continued, solving a set of linearized equations (18) for $\Delta\boldsymbol{\theta}_{n+\alpha}^{i}$ at every iteration step, until the solution converges to the non-linear solution.

The *quasi-stiffness* matrix $\hat{\mathbf{K}}_{n+\alpha}^{i}$ in (18) is a linearized tangential *stiffness matrix* which corresponds to the Jacobian matrix of the standard Newton-Raphson method, but in which the unsymmetrical term is neglected[3].

The convergence criteria employed is as follows:

$$\frac{\left\|\Delta\boldsymbol{\theta}_{n+\alpha}^{i}\right\|}{\left\|\boldsymbol{\theta}_{n+\alpha}^{i+1}\right\|} < TOL \tag{20}$$

where

TOL is the specified tolerance.

$\|\cdot\|$ denotes the Euclidean vector norm.

$\Delta\boldsymbol{\theta}_{n+\alpha}^{i}$ is the temperature change in the i^{th} iteration.

$\boldsymbol{\theta}_{n+\alpha}^{i+1}$ is the current temperature value.

2.2 Mechanical analysis

In the mechanical model, the onset of plastic behaviour is governed by a yield criteria dependent of stress level and from the plastic deformation by a general formula:

$$F(\sigma_{ij}, K, \theta) = f(\sigma_{ij}) - Y(K, \theta) \tag{21}$$

where, $f(\sigma_{ij})$ is a yield function; $Y(K, \theta)$, is a function that depends on a material hardening parameter, K, and the temperature, θ.

When the plastic flow occurs, the loading function will vary according to the equation:

$$dF = \frac{\partial F}{\partial \sigma_{ij}} d\sigma_{ij} + \frac{\partial F}{\partial K} dK + \frac{\partial F}{\partial \theta} d\theta = 0 \tag{22}$$

The flow rule governs the plastic flow after yielding and it will be assumed that the plastic strain incremental is proportional to the stress gradient of a plastic potential, so that:

$$d\varepsilon_{ij}^{p} = d\lambda \frac{\partial Q}{\partial \sigma_{ij}} \tag{23}$$

where Q is a plastic potential function and $d\lambda$ is the proportionality constant termed the plastic multiplier.

If the plastic potential is equal to the yield function, $f = Q$, equation (23) can be written as the associated theory of plasticity:

$$d\varepsilon_{ij}^{p} = d\lambda \frac{\partial f}{\partial \sigma_{ij}} \tag{24}$$

since it has been postulated that both are functions of $J_2^{'}$ and $J_3^{'}$.

2.2.1 The thermo-elastoplastic strain increment

The model is based upon the Prandtl-Reuss incremental plasticity theory[11]. Assuming small strains, the complete incremental relationship between stress and strain for thermo-elastoplastic deformation is found to be

$$d\varepsilon_{ij}^{t} = d\varepsilon_{ij}^{e} + d\varepsilon_{ij}^{p} + d\varepsilon_{ij}^{th} \tag{25}$$

The elastic strain increment is given by Hooke law:

$$d\varepsilon_{ij}^{e} = \frac{d\sigma_{ij}^{'}}{2\mu} + \frac{(1-2\nu)}{E}\delta_{ij}d\sigma_{kk} \tag{26}$$

The plastic strain increment is done by equation (24) and finally the thermal strain is done by

$$d\varepsilon_{ij}^{th} = \alpha(\theta)d\theta\delta_{ij} \tag{27}$$

where: $\alpha(\theta)$ is the thermal expansion coefficient, which can be temperature dependent.

The Von Mises yield criterion is formulated by the second deviatoric stress invariant, $J_2^{'}$, written as

$$\sqrt{3}(J_2^{'})^{1/2} = \sigma_y(K,\theta) \tag{28}$$

The incremental stresses occurring in the time interval are done:

$$d\sigma_{ij} = D_{ij}^{ep}d\varepsilon_{ij} + d\sigma_{th} = D_{ij}(d\varepsilon_{ij} - d\lambda a_j) + d\sigma_{th} \tag{29}$$

where D_{ij}^{ep} is the elastoplastique matrix.

The application of the virtual work principle gives finally the system of algebraic equations to be solved. This is done in the code FEMSEF98 using a modified Newton-Raphson method.

3 STEEL PROPERTIES ACCORDING TO THE EUROCODE 3

The thermal and mechanical properties of steel as function of the temperature shall be determined from the following.

3.1 Mechanical properties of steel

3.1.1 Strength and deformation properties

Figure 1 gives the reduction factors, relative to the appropriate value at 20ºC, for the stress-strain relationship for steel at elevated temperatures, as follows:

- effective yield strength, relative to yield strength at 20ºC: $k_{y,\theta} = f_{y,\theta} / f_y$
- slope of linear elastic range, relative to slope at 20ºC: $k_{E,\theta} = E_{a,\theta} / E_a$

At 20 ºC the Eurocode 1 gives the following values: $f_y = 235 \times 10^3\, kN/m^2$ and $E_a = 210 \times 10^6\, kN/m^2$.

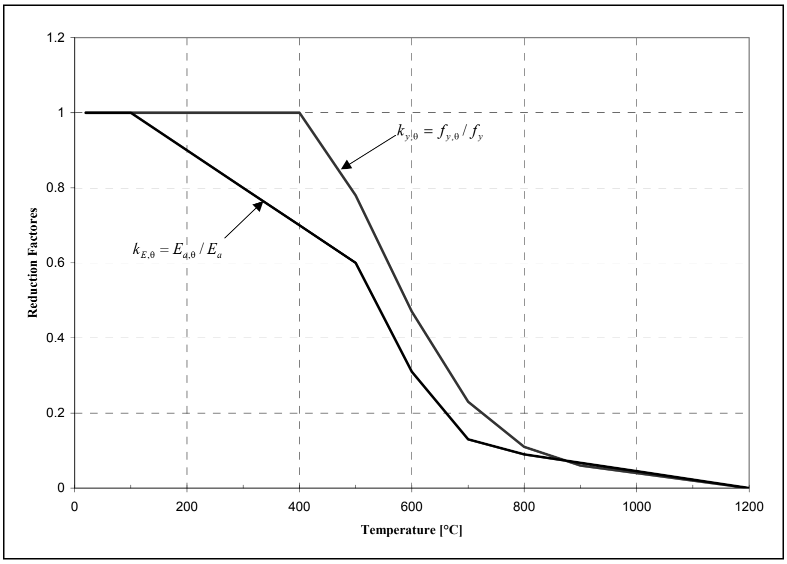

Fig. 1 – Dependency with temperature of the reduction factors $k_{y,\theta,com}$ and $k_{E,\theta,com}$

3.1.2 Unit mass

The unit mass of steel ρ_a may be considered to be independent of the temperature. The following value has been taken

$$\rho_a = 7850\, kg/m^3 \tag{30}$$

3.2 Thermal properties

3.2.1 Thermal elongation

Assuming a simple calculation model the relationship between thermal elongation and steel temperature may be considered to be constant, being the elongation determined from:

$$\Delta l / l = 14 \times 10^{-6} (\theta_a - 20) \tag{31}$$

3.2.2 Specific heat

The specific heat of steel c_a [JkgK], figure 2, may be determined from the following:

$$C_a = \begin{cases} 425 + 7.73\times10^{-1}\theta_a - 1.69\times10^{-3}\theta_a{}^2 + 2.22\times10^{-6}\theta_a{}^3 & 20^{\circ}C \le \theta_a < 600^{\circ}C \\ 666 + \dfrac{13002}{738-\theta_a} & 600^{\circ}C \le \theta_a < 7350^{\circ}C \\ 545 + \dfrac{17820}{\theta_a - 731} & 735^{\circ}C \le \theta_a < 900^{\circ}C \\ 650 & 900^{\circ}C \le \theta_a \le 1200^{\circ}C \end{cases} \quad (32)$$

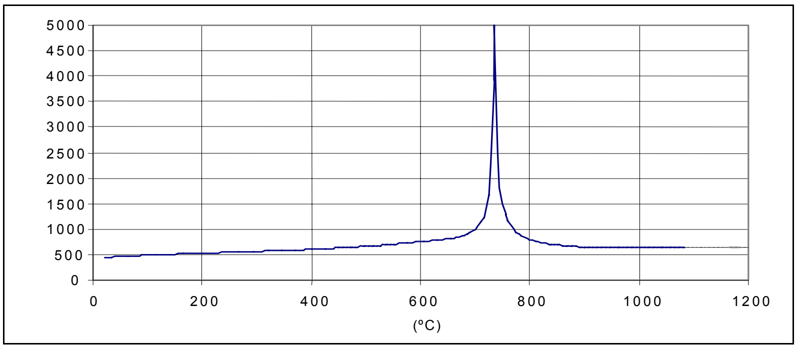

Fig. 2 – Dependency with temperature of the specific heat, [J/KgK]

3.2.3 Thermal conductivity

The thermal conductivity of steel λ_a [W/mK], figure 3, may be determined from the following:

$$\lambda_a = \begin{cases} 54 - 3.33\times10^{-2}\theta_a & 20^{\circ}C \le \theta_a < 800^{\circ}C \\ 27.3 & 800^{\circ}C \le \theta_a \le 1200^{\circ}C \end{cases}$$

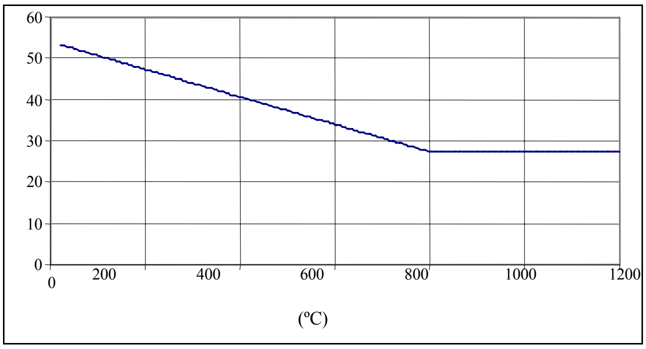

Fig. 3 – Dependency with temperature of the thermal conductivity, [W/mK]

4 STEEL TEMPERATURE DEVELOPMENT FOR UNPROTECTED INTERNAL STEELWORK

For an equivalent uniform temperature distribution in the cross-section, the increase of temperature $\Delta\theta_{a,t}$ in an unprotected steel member during a time interval Δt may be determined from [10]:

$$\Delta\theta_{a,t} = \frac{A_m / V}{c_a \rho_a} \dot{h}_{net,d} \Delta t \qquad (34)$$

where:

A_m / V - is the section factor for unprotected steel members, [m^{-1}];

A_m - is the exposed surface area of the member per unit length, [m^2/m];

V – is the volume of the member per unit length, [m^3/m];

c_a - is the specific heat of steel from (32) ,[J/kgK];

ρ_a - is the unit mass of steel, from (30), [kg/m^3];

$\dot{h}_{net,d}$ - is the design value of the net heat flux due to convection and radiation per unit area[9]:

$$\dot{h}_{net,d} = \gamma_{n,c}\dot{h}_{net,c} + \gamma_{n,r}\dot{h}_{net,r} \qquad [\mathrm{W/m^2}];$$

$\gamma_{n,c}$ - factor to account for different national types of test and equals [1.0]

$\gamma_{n,r}$ - is equal to [1.0] as $\gamma_{n,c}$;

$$\dot{h}_{net,c} = \alpha_c(\theta_g - \theta_m) \qquad [\mathrm{W/m^2}];$$

α_c - is the coefficient of heat transfer by convection, which must be taken[9] as 25 W/m^{2}K;

θ_g - is the gas temperature of the environment of the member in fire exposure.

In this work it was adopted the standard temperature-time curve ISO 834, which is given by:

$$\theta_g = 20 + 345\log_{10}(8t+1) \qquad [ºC];$$

t – time in minutes [min];

θ_m - surface temperature of the member;

$$\dot{h}_{net,r} = \Phi \cdot \varepsilon_{res} \cdot 5{,}67 \times 10^{-8} \cdot [(\theta_r + 273)^4 - (\theta_m + 273)^4] \qquad [W/m^2];$$

Φ - is the configuration factor, which should be taken[9] equals [1.0];

$\varepsilon_{res} = \varepsilon_m \cdot \varepsilon_f$ - is the resultant emissivity;

$\varepsilon_m = 0{,}625$ - is the emissivity related to the surface material[10];

$\varepsilon_f = 0{,}8$ - is the emissivity related to the fire compartment [9,10];

θ_r - is the radiation temperature of the environment of the member usually taken as $\theta_r = \theta_g$;

Δt - time interval, which should not be taken as more than 5 seconds[10].

5 THERMOMECHANICAL BEHAVIOUR OF STEEL COLUMNS EXPOSED TO THE STANDARD FIRE CURVE ISO 834

Results of the numerical modelling of the thermomechanical behaviour of hot-rolled profiles of the IPE, HEA, HEB and HEM series exposed to the standard fire curve ISO 834, acting on the four sides of the profile, as it can be seen in figure 4.a, are shown.

Due to the symmetry, only a quarter of the profile was analysed, being the finite element mesh used represented in figure 4.b.

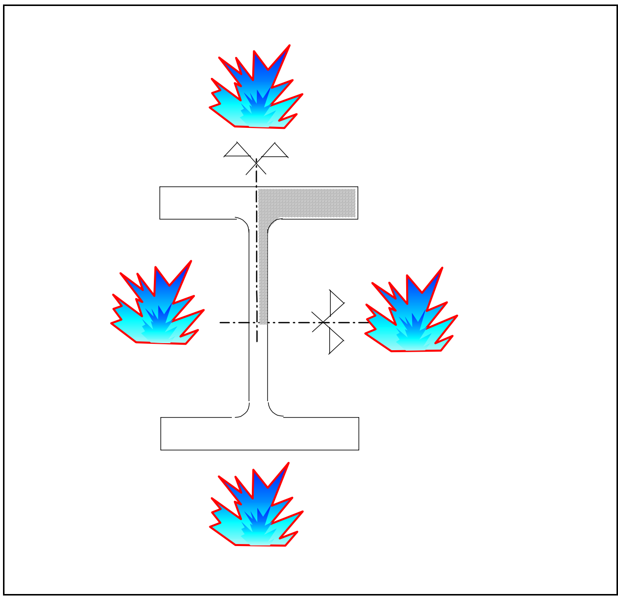

Fig. 4.a – Steel profile exposed to fire at four sides.

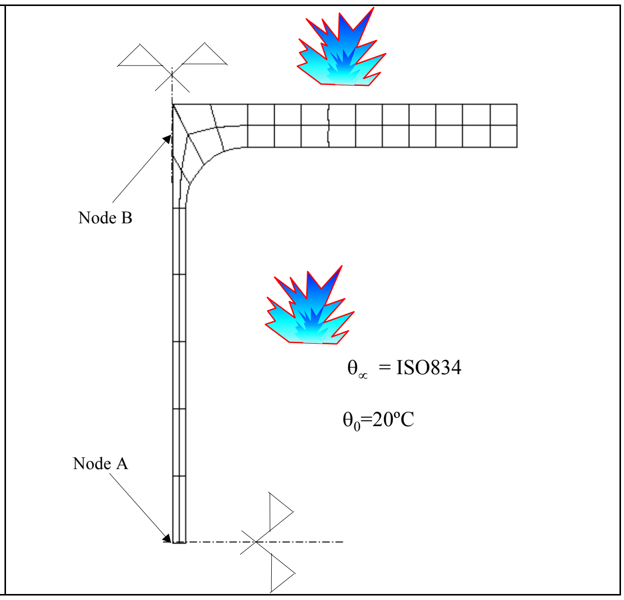

Fig. 4.b – Finite element mesh used.

In figure 5 we can see the variation of the section factor for all the profile series analysed in this paper.

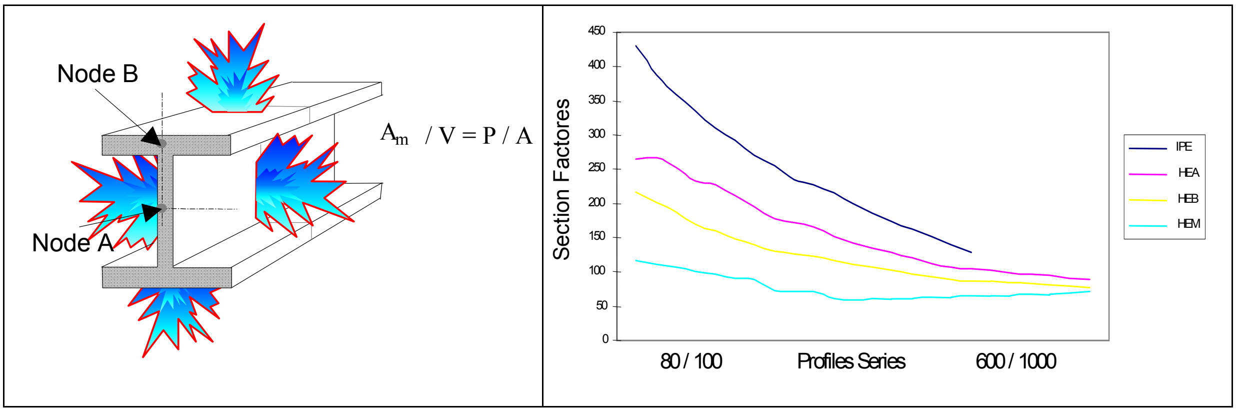

Fig. 5 – Section factors.

In figure 6 we can see the time history of temperature at node A and B for all profiles of the 400 series, using the simplified equation of the Eurocode 3 and the finite element results of FEMSEF98. It can be seen that the values of the temperature obtained from the Eurocode 3 equation are always between the values of the temperature of nodes A and B obtained using a finite element analysis. This shows that the values of the temperature of EC3 can be considered as an average value of the highest and lowest temperature in the profile.

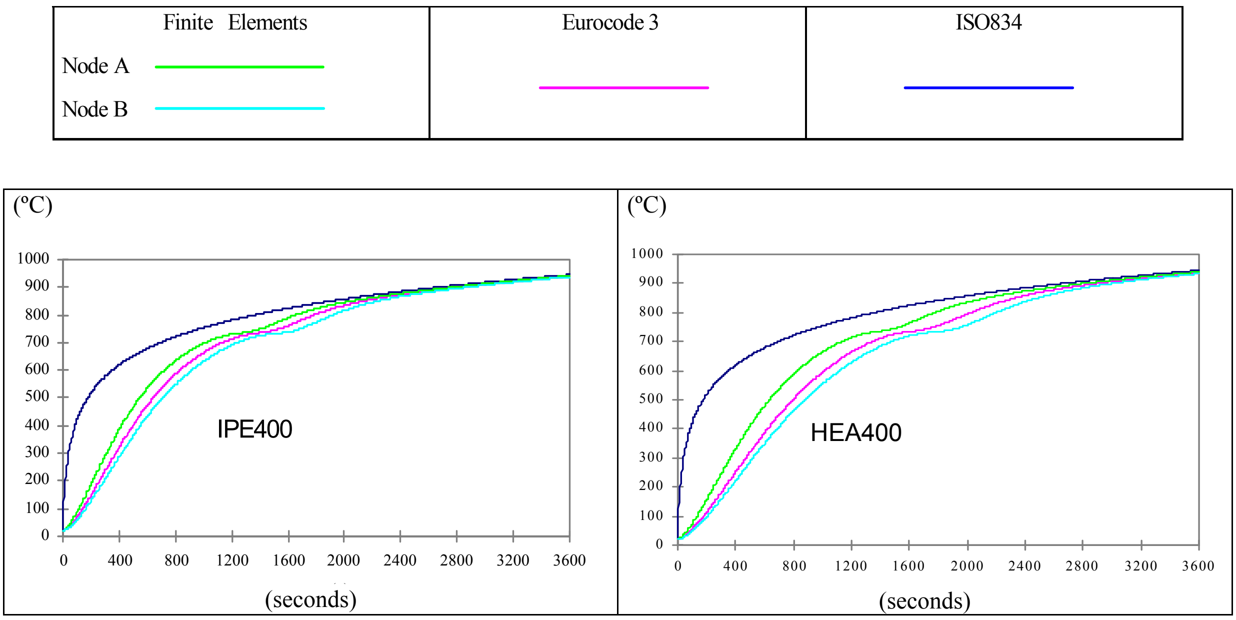

Fig. 6 – Time history of temperature of nodes A and node B (fig. 4) for all profiles series 400, obtained using the FEMSEF98 and the simplified Eurocode 3 equation.

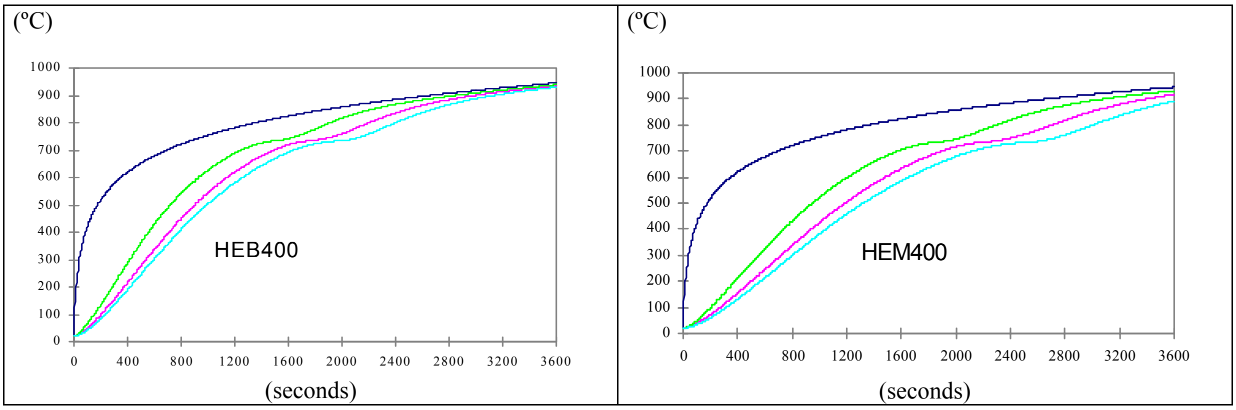

Fig. 6 – Time history of temperature of nodes A and node B (fig. 4) for all profiles series 400, obtained using the FEMSEF98 and the simplified Eurocode 3 equation.

Figure 7 shows the temperature evolution of node *A* for all the profile series, obtained using the finite element solver FEMSEF98. As the section factor decreases the temperature field, decreases too, with an exception of the profile series HEM.

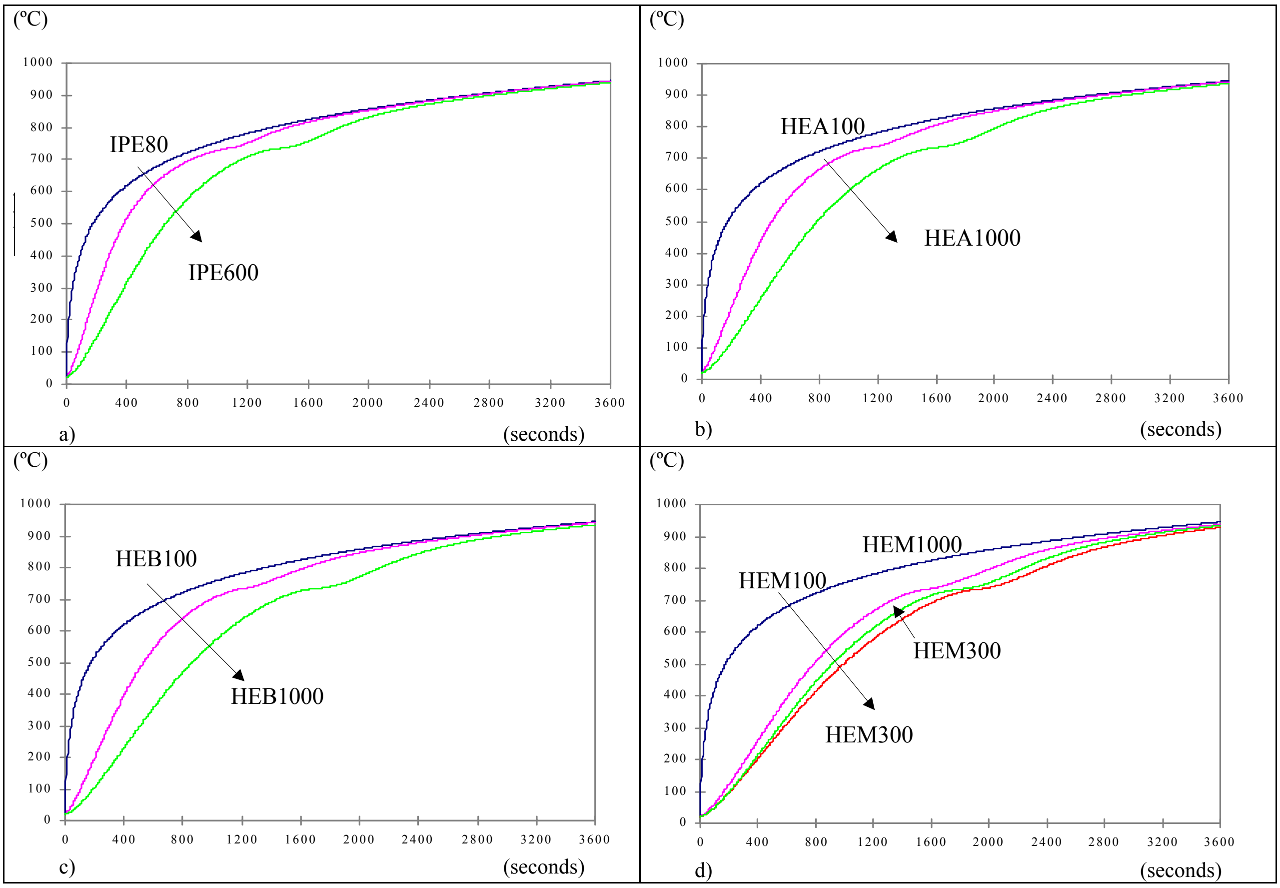

Fig. 7 – Time history of temperature of node A (fig. 4) for all profiles series and the ISO834: a) IPE, b) HEA, c) HEB, d) HEM.

Figure 8 shows the stress field for the time instant correspondent to the onset of the plastic behaviour in the size 400 of all the profile series, obtained by FEMSEF98 considering plane strain conditions. The numerical values in the boxes represent the time correspondent to the beginning of plastic behaviour in each 400 profile series.

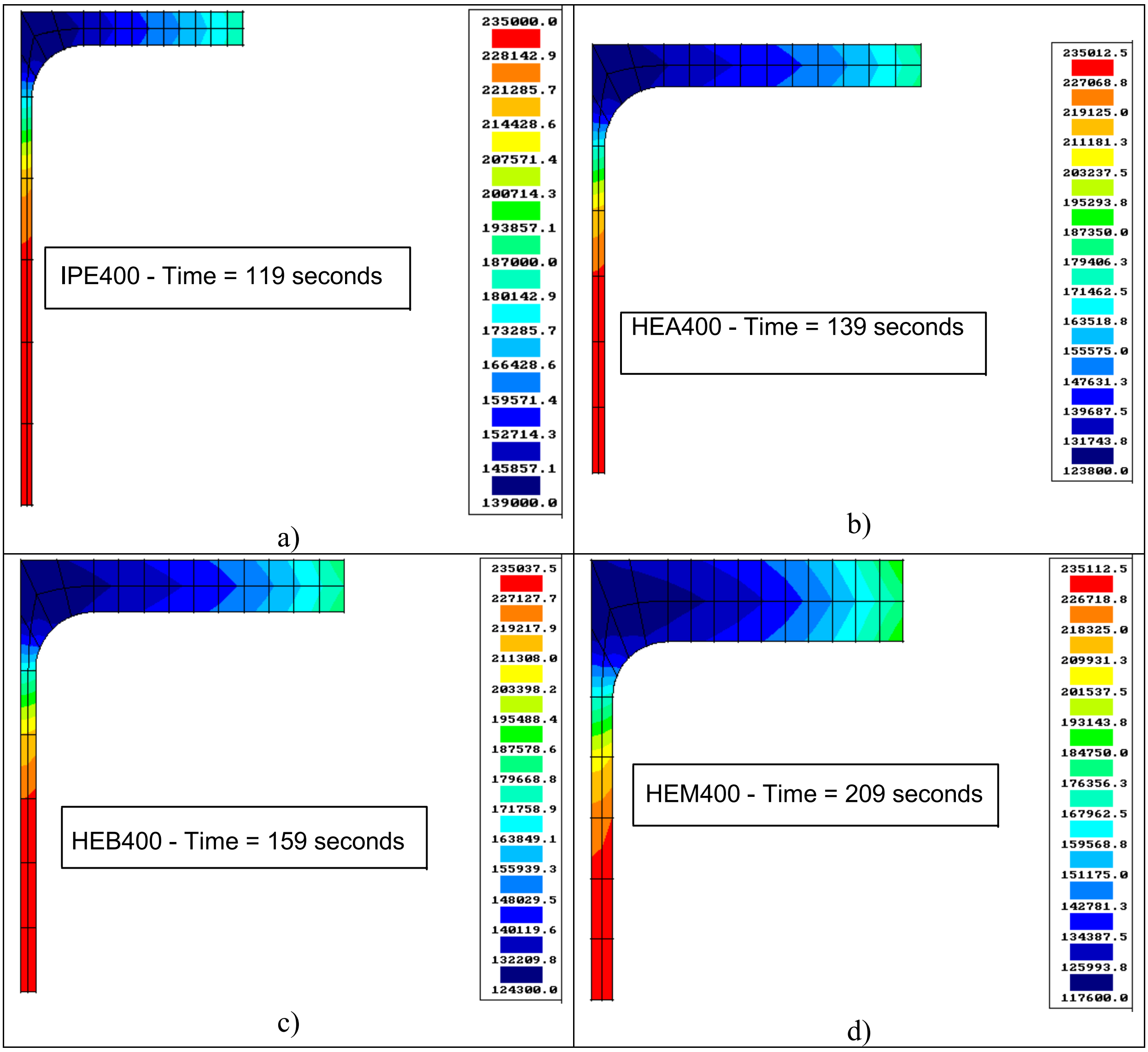

Fig. 8 – Equivalent stresses fields. a) IPE400; b) HEA400; c) HEB400; d) HEM400

Table 1 shows for several time instants after the beginning of the plastic behaviour, the lowest value of the equivalent stresses for all the profiles of Fig. 8.

Table 1

Profile	Section Factor [1/m]	Onset of plasticity [s]	σeq min	Time [s]	σeq min	Time [s]	σeq min
IPE400	174	119	139	120	143.2	126	152.8
HEA400	120	139	123.8	140	127.1	148	137.3
HEB400	97	159	124.3	160	127.3	164	131.1
HEM400	62	209	117.6	210	119.9	214	122.5

The same results are shown in table 2 for other profile series.

Table 2

Profile	Section Factor [1/m]	Onset of plasticity [s]	σeq min
IPE80	429	77	183.2
IPE400	174	119	139
IPE600	129	147	138.1
HEA100	264	97	152
HEA400	120	139	123.8
HEA600	89	178	115.4
HEB100	218	110	184.5
HEB400	97	159	124.3
HEB1000	78	195	115.4
HEM100	116	171	197
HEM400	62	209	117.6
HEM1000	70	208	115.1

6 CONCLUSIONS

A computational program based on the finite element method to model the thermo-elastoplastic behaviour of steel structural members exposed to the standard fire curve ISO 834 has been developed. This program has been used to study the thermo-mechanical behaviour of hot-rolled steel profile submitted to fire.

The results obtained with the developed program have been compared with the results obtained with the simplified heat conduction equation of the Eurocode 3. From this comparison we can conclude that the values of the temperature obtained from the Eurocode 3 equation are always between the values of the highest and lowest temperature obtained with the finite element analysis. The Eurocode results can be considered as an average of these two values.

It is possible to study the development of thermal stresses during the fire exposition, using the Eurocode material properties. With this information the designer can select the material and the profile to have an appropriate safety level or choose a thermal protection material if necessary.

ACKNOWLEDGEMENTS

This work was done within the framework of the project nº PBIC/C/CEG/2446/95 supported by FCT and entitled *"Numerical Modelling of Steel Structures Behaviour Under High Temperatures*".

REFERENCES

[1] E. M. M. Fonseca, *Numerical Modelling of Thermomechanical Behaviour of Hot-Rolled Steel Profiles Submitted to Fire*, MSc. Thesis (in Portuguese), University of Porto, FEUP,(1998).

[2] O.C. Zienkiewicz and K. Morgan, *Finite Elements and Approximation*, John Wiley & Sons, Inc., U. S. A., (1983).

[3] F. B. Damjanic, *Reinforced Concrete Failure Prediction Under Both Static and Transient Conditions*, Ph. D. Thesis, University College, Swansea, (1983).

[4] P. M. M Vila Real, *Finite Element Modelling of Thermo-Elastic Behaviour of Solids With High Thermal Gradients*, MSc. Thesis (in Portuguese), University of Porto, FEUP,(1988).

[5] P. M. M Vila Real, *Finite element modelling of the solidification and the thermomechanical behaviour of pieces poured on metallic moulds*, Ph. D. Thesis (in Portuguese), University of Porto, FEUP,(1993).

[6] T.J.R., Hughes, Unconditionally Stable Algorithms for Nonlinear Heat Condution*, Comp. Meth. Appl. Mech. Engng*., **10**, 135-139, (1977).

[7] O. C. Zienkiewicz and I. Cormeau, Viscoplasticity, Plasticity and Creep in Elastic Solids. A unified Numerical Solution Approach, *Int. J. Num. Meth. Engng*., **8**, 821-845, (1974).

[8] D. R. Owen, E. Hinton, *Finite Elements in Plasticity: Theory and Practice*, Pineridge Press, U. K., (1980).

[9] EUROCODE 1, Basis of Design and Actions on Structures - Part 2-2: Actions on Structures Exposed to Fire, ENV 1991-2-2, (1995).

[10] EUROCODE 3, Design of Steel Structures - Part 1-2: General Rules - Structural Fire Designe, ENV 1993-1-2, (1995).

[11] D. Assaker, J. C. Golinval, M. Hogce, M. Geradin, Termo-Plasticity Versus Termo-Viscoplasticity for Residual Stresses – Proceedings of 2nd International Conference on Computacional Plasticity - Part I: edited by: D. R. J. Owen, E. Hinton, E. Õnate, Pineridge Press, Swansea, Spain, 1989, pp. 501-514.